IOP Conf. Series: Materials Science and Engineering **167** (2017) 012038 doi:10.1088/1757-899X/167/1/012038

# Preparation, characterization and photocatalytic activities of $TiO_2$-$SrTiO_3$ composites

**Yan Wang, Lianjie Zhu[1], Fubo Gao and Hanjie Xie**

School of Chemistry & Chemical Engineering, Tianjin Key Laboratory of Organic Solar Cells and Photochemical Conversion, Tianjin University of Technology, Tianjin 300384, PR China.

E-mail: zhulj@tjut.edu.cn

**Abstract.** Series of $TiO_2$-$SrTiO_3$ composites were synthesized by hydrothermal method, using $TiO_2$ nanotube array as a precursor and $Sr(OH)_2$ as a Sr source material. $TiO_2$-$SrTiO_3$ products with various composition were obtained by simply changing the reaction time. The as-synthesized products were characterized by scanning electron microscopy (SEM) and X-ray diffraction (XRD). The optical properties were studied by means of UV-Vis absorption spectroscopy and photoluminescence (PL) spectra. Their photocatalytic activities were assessed by photodegradation of rhodamine B (RhB) solution and the photocatalytic reaction mechanism was discussed. The $TiO_2$-$SrTiO_3$ composites obtained at 2 h exhibits the highest activity for photodegradation of RhB.

## 1. Introduction

Nanostructured $TiO_2$ have attracted wide attention due to their high photocatalytic activity, low cost and excellent chemical stability [1-3]. Particularly, $TiO_2$ nanotube array film is a promising catalyst for photodegradations of organic pollutants because of its outstanding advantage in easy reclamation from a slurry system after photocatalytic reaction. However, pure $TiO_2$ (Eg=3.2 eV) can only absorb UV light and very little visible light, which limits the practical applications owing to the poor utilization of solar light [4,5]. Although cubic perovskite structure of $SrTiO_3$ (Eg=3.2 eV) also has large band energy, the $TiO_2$-$SrTiO_3$ composites could perform higher photocatalytic activity because of the difference in conduction and valence bands which could change migration process of photo-generated carriers, effectively promoting photo-generated electron-hole separation [6].

Many efforts have been devoted to the synthesis of $TiO_2$-$SrTiO_3$ heterostructure using hydrothermal method. For instance, $TiO_2$ powder was taken as a precursor to synthesize $TiO_2$-$SrTiO_3$ nanoparticles [7-10]. The other researchers [6,11-18] made use of $TiO_2$ nanotube array films as precursors to fabricate $TiO_2$-$SrTiO_3$ heterostructures. They mostly focus on the length and pore diameter of the $TiO_2$-$SrTiO_3$ composite nanotubes because longer nanotubes have larger surface areas enabling more light harvesting and more active sites accessible to pollutants in the aqueous environment [6]. However, the relations between reaction time and product morphology, composition and photodegradation activity have not been reported.

The present paper reports successful syntheses of the $TiO_2$-$SrTiO_3$ composites with different morphology and composition. The effects of reaction time on morphology, composition, crystal structure, optical property and photodegradation activity of the $TiO_2$-$SrTiO_3$ composites were

investigated systematically. The results show that photocatalytic activity of the $TiO_2$-$SrTiO_3$ composites are closely related with morphology and composition.

## 2. Experiment

$TiO_2$ nanotube array (NTA) precursor was synthesized as follows. In a typical procedure, a cleaned Ti foil (70 × 50 × 0.25 $mm^3$, 99.6% purity) was put into the electrolyte containing 1.0 g of $NH_4F$ in glycol solution with 3 vol.% $H_2O$ and 7 vol.% formamide, whose pH was adjusted to 4 by drop-wise addition of $H_2SO_4$. $TiO_2$ NTAs were obtained by potentiostatic anodization in a constant stirring two-electrode cell at 40 V for 2 h at room temperature with graphite as a counter electrode placed at 3 cm from the Ti foil. Then the as-obtained $TiO_2$ films were rinsed with ethanol and water for several times, dried at 60℃ in an oven. The $TiO_2$-$SrTiO_3$ composites were fabricated by a hydrothermal method. The anodized $TiO_2$ nanotube array films (25 × 13 $mm^2$) and 0.03 g strontium hydroxide ($Sr(OH)_2 \cdot 8H_2O$) was added to 20 mL deionized water in a Teflon stainless steel autoclave. The autoclave was sealed and heated to 150℃ in an oven for several hours. After it was cooled down to room temperature, the sample was removed from the autoclave, soaked in a 0.1 M HCl solution for 1 min, and rinsed with deionized water. Then the sample was calcined at 400℃ for 3 h in a muffle furnace with a heating rate of 5℃ $min^{-1}$. Consequently, series of $TiO_2$-$SrTiO_3$ composites were obtained.

X-ray diffraction (XRD) measurements were carried out on a Rigaku Ultima IV diffractometer) with a Cu K radiation source ( λ = 0.15418 nm) operated at 40 kV and 40 mA. The scanning electron microscope (SEM) were taken on Carl Zeiss MERLIN Compact scanning electron microscope and transmission electron microscope (Germany). The UV-vis diffuse reflectance absorption spectra were recorded on a Hitachi/U-3900 UV-visible spectrophotometer. The PL emission spectra were obtained from a F-7000 steady and time resolved spectrometer excited at 330 nm.

The photodegradation activities of the series of $TiO_2$-$SrTiO_3$ composites on RhB solutions were studied under simulated sunlight illumination. The $TiO_2$-$SrTiO_3$ composites was horizontally placed at the bottom of a 10 mL of beaker with the nanotubes upwards. Then 8 mL of 0.01 g $L^{-1}$ RhB aqueous solution was put into above beaker, which was in dark sonicated for 30 min and air bubbled for another 30 min to reach adsorption-desorption equilibrium. The catalytic system was then exposed to the simulated sunlight irradiation from a 400 W halogen light (5% UV light) located 15 cm above the solution and kept air bubbling during the whole photodegradation reaction. The concentration of the RhB solution at certain time interval was determined by measuring its absorbance at 552 nm on a UV-visible spectrophotometer, from which the photodegradation rate was expressed by $(A_0\text{-}A)/A_0$, where $A_0$ is the initial absorbance of the RhB solution and A is the absorbance at certain reaction time.

## 3. Results and discussion

### *3.1. Morphology and crystal structure*

The surface and lateral SEM images of the as-anodized $TiO_2$ films and $TiO_2$-$SrTiO_3$ composites obtained at different reaction time show that they are mostly well-aligned nanotube arrays, grown vertically from Ti substrates (figure.1). As shown in figure.1(A), the pure $TiO_2$ film was composed of ordered nanotubes with an average diameter and tube length of about 106.8 nm and 3.1 μm, respectively. The formation of $TiO_2$ NTAs in fluorinated electrolyte was the result of three simultaneously occurring processes [19]: (1) field-assisted oxidation of Ti metal to $TiO_2$ ($Ti + H_2O \rightarrow TiO_2+H_2$), (2) field-assisted dissolution of Ti metal into electrolyte ($Ti + 6HF + 2H^+ \rightarrow [TiF_6]^{2-}+2H_2$) and (3) chemical etching of $TiO_2$ to $TiF_6^{2-}$ ($TiO_2 + 6F^- + 4H^+ \rightarrow [TiF_6]^{2-}+ 2H_2O$).

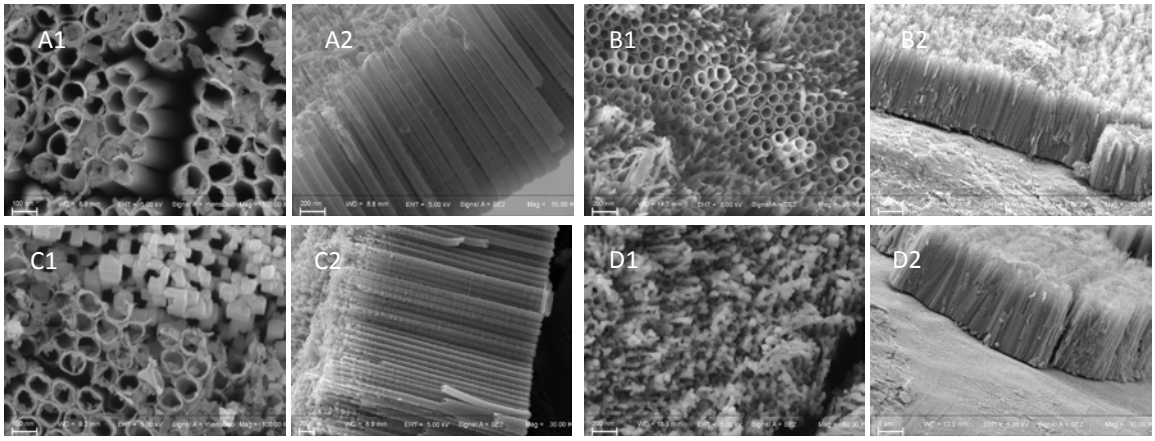


**Figure 1.** SEM images of $TiO_2$-$SrTiO_3$ composites obtained at different reaction times: (A) 0 h, (B) 2 h, (C) 3 h and (D) 6 h

It is noticed that the morphology of the $TiO_2$-$SrTiO_3$ composites change with prolonging reaction time (especially the surface morphology) although the tubular structure of the $TiO_2$ precursor was remained mostly (figure. 1B-D). When the reaction time is 2 hours (figure. 1B), the nano-tubular structure of the product was well preserved and mouths of the tubes became clear, which may be due to the transformation reaction from $TiO_2$ to $SrTiO_3$. This implies the specific surface area of the sample obtained at 2 h remained high. After 3 h reactions, $SrTiO_3$ nanocubes were partly dispersed on the nanotube surface and interior, as shown in figure.1(C), suggesting that the specific surface area of this $TiO_2$-$SrTiO_3$ composite was decreased. Further prolonging the reaction time to 6 h led to formation of more nanocubic $SrTiO_3$ which covered the whole surface of $TiO_2$ nanotubes. Thus, the tubular structure of the product became obscure from top surface view and the specific surface area was further decreased. Thus, the $TiO_2$-$SrTiO_3$ composite obtained at 2 h may possess the largest specific surface area which would lead to more active sites available for adsorption of dyes on their surfaces [20].

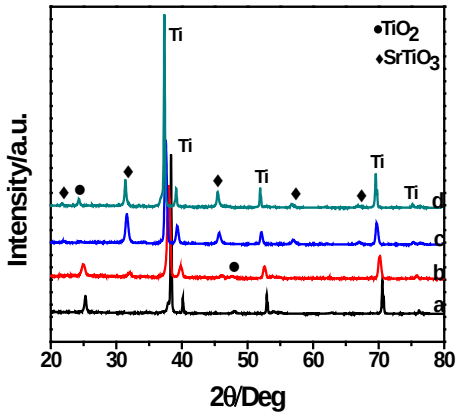


**Figure 2.** XRD patterns of $TiO_2$-$SrTiO_3$ composites prepared at different reaction times: (a) 0 h, (b) 2 h, (c)3 h and (d) 6 h

On the basis of these results and literature [13], we propose a formation mechanism of $TiO_2$-$SrTiO_3$ composites, which can be hypothetically described as follows: (i) $TiO_2$ molecules were dissolved by hydroxyl radicals ($OH^-$) to generate $[Ti(OH)_6]^{2-}$ ions ($TiO_2 + 2OH^- + 2H_2O \rightarrow [Ti(OH)_6]^{2-}$), (ii) more and more as-formed $[Ti(OH)_6]^{2-}$ ions further reacted with $Sr^{2+}$ to generate

$SrTiO_3$ nanoparticles on the surface of $TiO_2$ nanotubes ($Sr^{2+} + [Ti(OH)_6]^{2-} \rightarrow SrTiO_3 + 3H_2O$). With the reaction proceeding, more and more $TiO_2$ were converted to $SrTiO_3$ and nanocube morphology occurred on the surface layer, so that the nanotube structure can no longer be maintained at the surface layer. The SEM results also support that the transformation reaction from $TiO_2$ nanotubes to $SrTiO_3$ nanostructures were proceeded from surface to Ti substrate. Therefore, only top layers of $TiO_2$ nanotubes were converted to $SrTiO_3$ nanostructures and down layers of $TiO_2$ nanotubes closed to the Ti substrate were remained. Consequently, the as-obtained products from 2-6 h are all $TiO_2$-$SrTiO_3$ composites which are proven by the following XRD results.

The XRD pattern of the as-obtained pure $TiO_2$ nanotube array film (figure. 2a) shows that except the diffraction peaks of the Ti substrate, two peaks of a tetragonal anatase $TiO_2$ at $2\theta$ = 25.3° and 48.0° are observed, corresponding to (101) and (200) planes (JPCDS: 21-1272, space group: I41/amd (141), cell: a = 3.785 Å, b = 3.785 Å, c = 9.514 Å). For the $TiO_2$-$SrTiO_3$ composites obtained at different reaction times (Fig. 2b-d), however, other five peaks of a tausonite $SrTiO_3$ at $2\theta$ = 22.8°, 32.4°, 46.5°, 57.8° and 67.8° are observed, corresponding to (100), (110), (200), (211) and (220) planes (JPCDS: 05-0634, space group: Pm-31[221], cell: a = b = c =3.905 Å). All diffraction lines of $TiO_2$ and $SrTiO_3$ are sharp and narrow, indicating a high crystallinity of the $TiO_2$-$SrTiO_3$ composites. With prolonging the reaction time, the peak intensities of the $SrTiO_3$ phase gradually increased, whereas the peaks of $TiO_2$ gradually weakened. These results indicate that the $TiO_2$ nanotubes were gradually converted to $SrTiO_3$ and the phase ratio of $SrTiO_3$:$TiO_2$ gradually increased. $SrTiO_3$ became dominant phase after 3 h's reaction. However, when the reaction time is 2 h, the $TiO_2$ phase was still predominant in the presence of $TiO_2$-$SrTiO_3$ heterostructure, which may result in the higher photocatalytic activity.

### *3.2. Optical peoperties of $TiO_2$-$SrTiO_3$ composites*

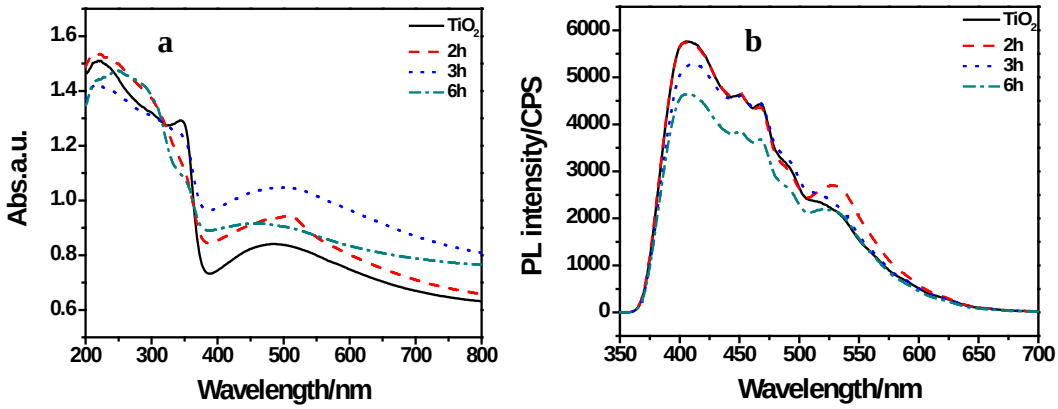


**Figure 3.** (a) UV-Vis diffuse reflection absorption spectra and (b) Photoluminescence spectra of $TiO_2$-$SrTiO_3$ composites prepared by hydrothermal method for different reaction time

The optical properties of the $TiO_2$-$SrTiO_3$ composites obtained at different reaction time were investigated by UV-vis diffuse reflectance absorption spectra and PL spectra. As shown in figure.3(a), a strong absorption band in UV light region and a relatively weaker absorption band in visible light region were present for each $TiO_2$-$SrTiO_3$ composite sample, which are similar to that of the pure $TiO_2$ nanotube array film except that the absorptions to visible light are enhanced significantly. With increasing reaction time, the absorption peak intensities of the $TiO_2$-$SrTiO_3$ composites in the visible light region firstly increase and then decrease. These results indicate that the $TiO_2$-$SrTiO_3$ heterostructures could greatly enhance the absorption to visible light and thus may effectively increase the photocatalytic activity of the catalyst. For $TiO_2$-$SrTiO_3$ heterostructures, the photo-generated

electron could transfer from conduction band (CB) of $SrTiO_3$ to conduction band (CB) of $TiO_2$. At the same time, the holes on valence band of $TiO_2$ could transit to valence band of $SrTiO_3$. This maybe make $TiO_2$-$SrTiO_3$ composites absorb light in longer wavelength, resulting in enhanced absorption of $TiO_2$-$SrTiO_3$ composites on visible light.

The PL spectra in figure. 3(b) demonstrate that the emission bands of the $TiO_2$ NTAs and $TiO_2$-$SrTiO_3$ composites are all in the range of 380-600 nm with peak values at around 410 nm. The PL peak intensity of the $TiO_2$-$SrTiO_3$ composite obtained at 2 h is similar to that of the pure $TiO_2$ NTAs, except the peak at around 530 nm, which may be caused by the $TiO_2$-$SrTiO_3$ heterostructure, suggesting that $TiO_2$-$SrTiO_3$ heterostructure with suitable phase ratio is beneficial to separation of photo-generated electrons and holes, which may result in higher photocatalytic activity.

### *3.3. Photodegradation activities on RhB and reaction mechanism*

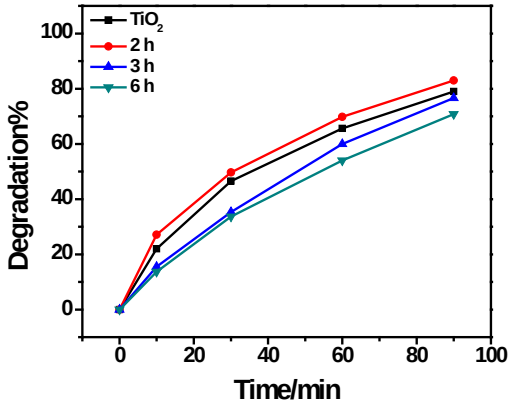


**Figure 4.** Photocatalytic performance of $TiO_2$-$SrTiO_3$ composites obtained at different reaction time on rhodamine B

Figure.4 demonstrates the photocatalytic performance of the $TiO_2$ NTA films and $TiO_2$-$SrTiO_3$ composites on RhB dye. With prolonging the illumination time, the photodegradation percentages of RhB over the series of catalysts increase gradually and reach 83% at 90 min for the best catalyst. With increasing the hydrothermal time, the photodegradation rate of RhB over the $TiO_2$ NTAs and $TiO_2$-$SrTiO_3$ composites firstly increased, reaching maximum and then decreased gradually. The $TiO_2$-$SrTiO_3$ composite obtained at 2 h possesses the highest photocatalytic activity, which may be attributed to its high specific surface area, $TiO_2$-$SrTiO_3$ heterostructure with mostly $TiO_2$ phase and enhanced visible light absorption ability.

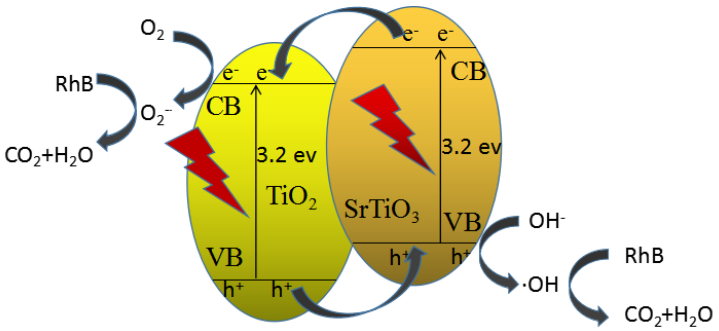


**Figure 5.** Schematic illustration of the reaction mechanism of photodegradation of RhB over the $TiO_2$-$SrTiO_3$ composites.

The possible photocatalytic reaction mechanism could be as follows. As shown in figure.5, under illumination, $TiO_2$ and $SrTiO_3$ generate photo-generated electron and holes. And then the photo-generated electron ($e^-$) could transfer from conduction band (CB) of $SrTiO_3$ to conduction band (CB) of $TiO_2$. At the same time, the holes ($h^+$) on valence band of $TiO_2$ could transit to valence band of $SrTiO_3$. The holes can oxidize RhB or react with $OH^-$ or water to form hydroxyl radicals (·OH). Electrons ($e^-$) in the conduction band (CB) reduces dissolved molecular oxygen to create superoxide ($O^{2-}$). RhB in the solution then are degraded by hydroxyl radicals (·OH) and superoxide anions ($O^{2-}$) to inorganic compounds of $CO_2$ and $H_2O$ [6]. In order to achieve maximum photodegradation efficiency, high visible light absorption ability and rapid charge separation, originated from $TiO_2$-$SrTiO_3$ heterostructure with suitable phase ratio, is desired. Besides, a large active surface area is also an important factor because more active sites are available for photocatalytic reactions. The $TiO_2$-$SrTiO_3$ composites obtained at 2 h has more surface active sites, strong visible light absorption capability and good photo-generated electrons/holes separation due to suitable composition of $SrTiO_3$, resulting in the highest activity for photodegradation of RhB.

## 4. Conclusion

Series of $TiO_2$ NTA-$SrTiO_3$ composites with different phase ratio have been successfully prepared by a facile hydrothermal method. With prolonging hydrothermal time, $TiO_2$ nanotubes are firstly converted to $SrTiO_3$ nanotubes with remained high specific surface area. Then $SrTiO_3$ nanocubes appear on the surface layer of the $TiO_2$ nanotube and gradually expand toward Ti substrate, accompanying with phase transformation from $TiO_2$ to $SrTiO_3$. When the hydrothermal time is 2 h, the obtained $TiO_2$ NTA-$SrTiO_3$ composite possesses high surface area (more active sites) with $TiO_2$ as the main phase which exhibits the highest activity for photodegradation of RhB. Optical studies of the series of samples indicate the high photocatalytic activity may be also related with its high visible light absorption and good separation of the photo-generated electrons/holes originated from suitable $TiO_2$-$SrTiO_3$ heterostructure.

## References

[1] Liu Y, Wang Z, Wang W and Huang W 2014 *J. Catal.* **310** 16
[2] Yang X, Qin J, Li Y, Zhang R and Tang H 2013 *J. Hazard. Mater.* **261** 342
[3] Zheng W, Liu X, Yan Z and Zhu L 2009 *ACS Nano* **3** 115
[4] Cesano F, Bertarione S, Damin A, Agostini G, Usseglio S and Vitillo J G 2008 *Adv. Mater.* **20** 3342
[5] Kitano M, Matsuoka M, Ueshima M and Anpo M 2007 *Appl. Catal. A* **325** 1
[6] Zhang X, Huo K, Hu L, Wu Z and Chu P 2010 *J. Am. Ceram. Soc.* **93** 2771
[7] Ruzimuradov O, Nurmanov S, Hojamberdiev M, Prasad R M, Gurlo A, Broetz J, Nakanishi K and Riedel R 2014 *Mater. Lett.* **116** 353
[8] Yue X, Zhang J, Yan F, Wang X and Huang F 2014 *Appl. Surf. Sci.* **319** 68
[9] Yan J, Zhu Y, Tang Y and Zheng S 2009 *J. Alloys Compd.* **472** 429
[10] Wang T, Liu S and Chen J 2011 *Powder Technol.* **205** 289
[11] Zhu Y, Xu L, Hu J, Zhang J, Du R and Lin C *2014 Electrochim Acta* **121** 361
[12] Yang Y, Lee K Y, Kado Y and Schmuki P 2012 *Electrochem Commun.* **17** 56
[13] Huang J, Tan X, Yu T, Zhao L and Hu W 2014 *Electrochim Acta* **146** 278
[14] Zhou J, Yin L, Li H, Liu Z, Wang J, Duan K, Qu S, Weng J and Feng B 2015 *Mater.Sci. Semicond.Process.* **40** 107
[15] Zhang Y, Bu Y, Yu J and Li P 2013 *J Nanopart Res* **15** 1717
[16] Jiao Z, Chen T, Yu H, Wang T, Lu G and Bi Y 2014 *J. Colloid Interface Sci.* **419** 95
[17] Wu Z, Su Y, Yu J, Xiao W, Sun L and Lin C 2015 *Int. J. Hydrogen Energy* **40** 9704
[18] Guo L, Wang X, Zhang H and Li L 2013 *Ceram. Int.* **39** S633
[19] Lai C W and Sreekantan S 2011 *J. Nanomater.* **2011** 99
[20] Alsawat M, Altalhi T, Shapter J and Losic D 2014 *Catal Sci. Technol.* **4** 2091